Easy teaching of numerical simulation of welding with COMSOL

I. Tomashchuk*[1], P. Sallamand[1], J.-P. Chateau-Cornu[2]
1 Laboratoire Interdisciplinaire Carnot de Bourgogne UMR CNRS 6303, Université de Bourgogne Franche-Comté, 12 rue de la Fonderie, 71200 Le Creusot, France
2 Laboratoire Interdisciplinaire Carnot de Bourgogne UMR CNRS 6303, Université de Bourgogne Franche-Comté, Institut Maray-Maison de la Métallurgie, 64 rue de Sully, 21000 Dijon, France
* iryna.tomashchuk@u-bourgogne.fr

Abstract

The initiation in numerical modeling of welding with COMSOL Multiphysics is proposed to the 2nd year students of the Professional Master Program «Processes, Controls, Metallic Materials: Nuclear Industry» (PC2M) of University of Burgundy, France since 2016 within the module «Simulation of welding physics». This training follows transversal aims such as easy comprehension of the influence of operational parameters on weld properties, learning different kinds of physical phenomena of welding and getting hands-on experience in creation of multiphysical models.
We hope that this course will promote the culture of multiphysical modeling amongst young specialists in the manufacturing of metallic parts and structures, in particular for the nuclear industry.

Introduction

The popularization of numerical simulation methods for apprehending the problems of materials processing, and in particular the quality of welding, in industry as well as in research, makes it necessary to create sufficient baggage of knowledge for new generations of specialists in materials science. In this light, COMSOL Multiphysics represents an interesting pedagogical tool that allows recreating and understanding the principles of relatively complex models without important prior background in programming and numerical methods.
Practical works in simulation of welding with COMSOL Multiphysics have been proposed to the 2nd year students of the Professional Master Program «Processes, Controls, Metallic Materials: Nuclear Industry» (PC2M) of University of Burgundy, France created in 2015, which is a unique professional training dedicated to the metallurgy in France [1]. The module «Simulation of welding physics». This training follows three transversal aims:

1. hands-on experience of creation, solving and post-processing of multiphysical models;
2. better understanding of coexistent physical phenomena of welding and their synergetic effect;
3. easy comprehension of the influence of operational parameters and materials properties on resulting weld.

These practical works are composed by four sessions of 3 hours each, dedicated to the creation of models of increasing complexity:

1. comparison of time-dependent and quasi-steady formulations of welding problem in Heat Transfer module;
2. performing the parametrical studies of input parameters (material properties, welding velocity etc.) influence on melted zone dimensions;
3. simulation of several convection forces and the analysis of their synergetic effect on melted zone dimensions and temperature (strong coupling between CFD and Heat Transfer modules);
4. modeling of elements transport in the melted zone (strong coupling between CFD, Heat Transfer and Diluted Elements Transport modules).

Theoretical content and step-by-step description of models creation along with efficient post-processing tips are provided in form of richly illustrated work-book of 40 pages. The students work in a pair and are evaluated basing on the reports that contain a short description of modeling steps and a vast discussion dedicated to the understanding of simulated phenomena and their impact on calculated thermal, velocity or composition fields as well as to the associated numerical challenges (effect of mesh size, stabilization, solving of convergence problems). The calculations are performed with pedagogical license of Calculation Center of University of Burgundy. For the reason of limited work time, the validation of the models by comparison with experimental results is not treated; however, it can be performed in case of more extended works such as individual research project for obtaining Master's degree.
This practical course is associated with 1-hour explanation of theoretical setup of each proposed model and preceded by 4 h of lectures on numerical simulation of welding given by two academicals and one invited R&D specialist.
The following paragraphs will resume the content and main outcome of the proposed models.

Practical work 1 (PW1): main principles of heat-transfer simulation in welding

During the first practical work, the students discover the interface of COMSOL Multiphysics and Heat Transfer module and go through the steps of setup, solving and post-processing of heat equation based models. 3D model with simplest Gaussian heat source applied to the top limit of the geometry is used (Q_{surf}). Two approaches to the representation of the welding process are compared:

1. quasi-steady approach where the heat source itself does not include velocity term, but the displacement of the welded plate is taken in account through the convective term of heat equation given in stationary form [2]

$$Q_{surf} = \frac{\eta \cdot P}{\pi \cdot R^2} \exp\left(-0.5 \frac{(x^2+y^2)}{R^2}\right)$$

$$\rho C_p \cdot \begin{bmatrix} 0 \\ V \\ 0 \end{bmatrix} \cdot \nabla T = \nabla \cdot (k \nabla T)$$

2. time-dependent approach with moving heat source and zero convective field in heat transfer equation:

$$Q_{surf} = \frac{\eta \cdot P}{\pi \cdot R^2} \exp\left(-0.5 \frac{(x^2+(y+V \cdot t)^2)}{R^2}\right)$$

$$\rho C_p \frac{\partial T}{\partial t} + \rho \cdot C_p \cdot \begin{bmatrix} 0 \\ 0 \\ 0 \end{bmatrix} \cdot \nabla T = \nabla \cdot (k \nabla T)$$

where η - efficiency coefficient, R – heat source radius, P – laser power, ρ - material density, Cp – heat capacity, k – thermal conductivity, V – welding speed, T – temperature, t – time.

The choice of limit conditions for two cases is discussed. In the first place, the thermophysical properties of materials from Materials Library are considered (AISI304L stainless steel). The influence of mesh size on the precision of calculated thermal field is demonstrated by the series of calculation with more and more thin domain mesh.

In the post-processing part, the students are invited to compare melted zone shapes and thermal gradients produced by two models, that appear to be very close when steady regime is attained by time-dependent model (Figure 1). The students learn to produce animations, extract melted zone (MZ) length and volume.

Practical work 2 (PW2): role of materials properties and parametric studies

The second practical work is dedicated to various parametric studies in quasi-steady 3D model:

- the influence of materials properties on melted zone dimension (by comparison of different materials from Materials Library)
- the influence of the quality of introduced material data (constant values, functions of temperature, taking in account latent heat of fusion)
- the influence of welding speed on melted zone dimensions.

In the first place, the students are invited to compare the shape and the dimensions of the melted zones produced by the same welding condition (fixed power and velocity) on different metallic materials and correlate them with melting temperatures T_m and thermal diffusivities α (Table 1).

Table 1. Melted zone widths produced on 2 cm thick plates with Gauss heat source with P = 10 kW, Ø = 1 cm, η = 0.7 and V = 0.5 m/min.

Material	T_m (K)	α (m²/s)	MZ width (mm)
AISI 304L	1673*	11.9	22.0
Ti	1928	11.2	23.7
Al	933	88.5	30.6
Cu	1356	113	19.4
Sn	510	40.8	33.2

*solidus temperature

Next, the calculation of thermal field on 16 MnNiMo 5 steel is performed:

- with constant properties,
- with properties as function of temperature and latent heat of fusion taken into account through equivalent heat capacity approach [3]:

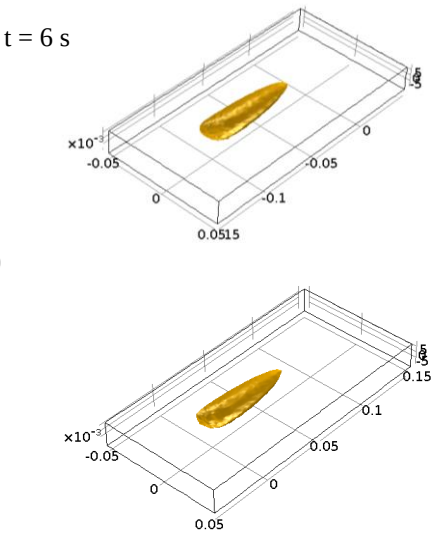

Figure 1. The comparison of 1673 K (solidus of 304L) isotherm for time-dependent (a) and quasi-steady (b) models of heat source.

$$C_p = C_p(T) + L_m \cdot \frac{e^{\frac{-(T-T_m)^2}{\Delta T^2}}}{\sqrt{\pi \Delta T^2}}$$

where $Cp(T)$ – heat capacity as function of temperature, L_m – latent heat of fusion, T_m – melting temperature, ΔT – smoothing range.

The dimensions of melted zone and thermal history along the joint line are compared (Figure 2) to highlight the importance of correct data for accurate simulation of melted zone length and cooling temperatures.

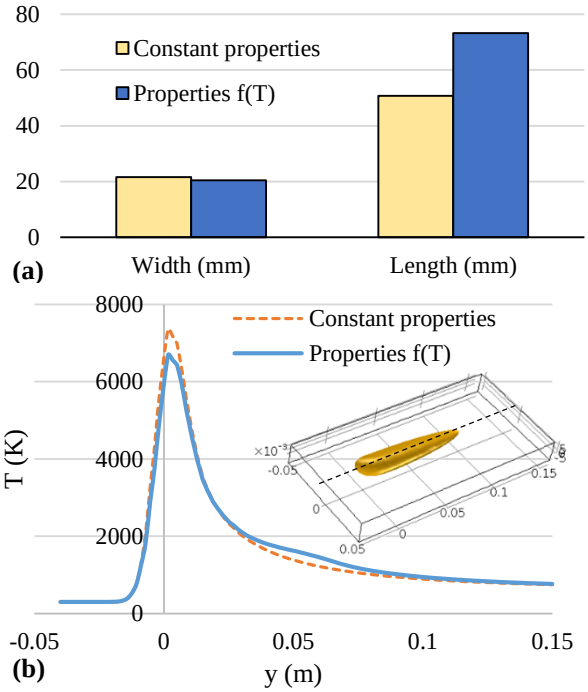

Figure 2. The dimensions of melted zone (a) and thermal history at the top of the joint line (b) compared for constant and temperature-dependent material properties.

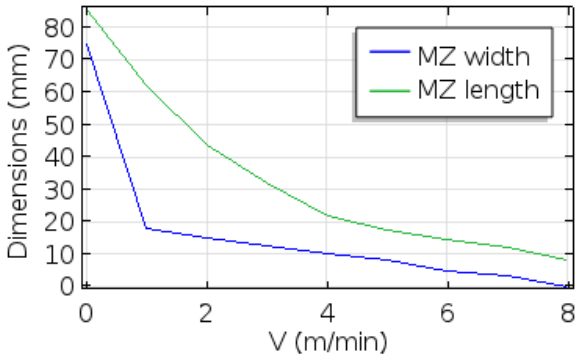

Figure 3. The effect of welding speed on melted zone dimensions of 16MND5, P = 10 kW, Ø = 1 cm, η = 0.7 and V = 0.5 m/min.

Finally, the parametric study of the influence of welding speed on melted zone dimensions is performed (Figure 3). It can be noticed that the melted zone length is more sensible to the welding speed than melted zone width.

Practical work 3 (PW3): convective forces in welding

Previously considered heat transfer models do not provide a correct description of thermal field within the melted zone because of neglecting of convective forces that strongly influence the melt temperatures, which remains unrealistic (~10000 K) in purely thermal models. In two next practical works, the students learn to introduce to the 2D model two convective forces that are common for all fusion-welding methods:

- natural convection through Boussinesq approximation [4]

$$F_A = -g \cdot \rho \cdot \beta \cdot (T - T_m)$$

where F_A – Archimedes force, g – gravity constant, β - thermal expansion coefficient;

- Marangoni convection created by the variation of surface tension σ with temperature [5] :

$$\sigma(T) = \sigma_m + \gamma_M \cdot (T - T_m)$$

where γ - surface tension temperature coefficient.

In these models, melted metal is represented as Newtonian liquid undergoing laminar flows. The strong coupling between the heat and Navier-Stokes equations is applied, because from one side density and viscosity are temperature-dependent functions and from other side heat equation contains, in contrary to the previous models, complete velocity field U(u,v):

$$\rho C_p \cdot U \cdot \nabla T = \nabla \cdot (k \nabla T)$$

$$\rho (U \cdot \nabla) U = \nabla \cdot \left[-pI + \mu \left(\nabla U + (\nabla U)^T \right) \right] + F_A$$

$$\rho \nabla \cdot (U) = 0$$

where p - relative pressure, I – identity tensor, μ - dynamic viscosity.

The equivalent viscosity approach is used, where very high value capable to suppress any velocity field is applied to the solid part of domain:

$\mu = \mu_{solid} + (\mu_{liquid} - \mu_{solid}) \cdot flc2hs(T - T_m, \Delta T)$,

where *flc2hs()* – a smoothed Heaviside function with a continuous second derivative without overshoot.

This model represents the simplified case when the defocused laser beam is applied on the surface of metallic material with high thermal conductivity, and the thermal equilibrium is attained, which means the melted zone does not evolve with time. The students observe the evolution of velocity fields (Figure 4) and maximal melt temperatures (Table 2) along with melted zone dimensions and the direction of the flows.

This study helps better understand the influence of the absolute value and the sign of γ on the resulting shapes of the melted zones. The students create in the first place steady heat transfer model and note maximal temperature and dimensions of the melted zone produced by defocused laser beam on the metal plate. Next, the natural convection is activated, and its impact on heat transfer is evaluated. It can be seen that quite slow velocity field created by natural convection does not affect the temperature and the dimensions of the melt. Then the Marangoni convection is activated. For given conditions, it results in maximal melt velocity of about 1 m/s. Negative sign of γ results in melt convection from the hot center to the periphery of the melted zone, that reduces maximal temperature (-40 K) and produces larger and less deep melted zone. Positive sign of γ inverses the direction of the flows : colder liquid comes from the periphery of the melt to its center, and hot liquid descends at the bottom of the melt, which results in slightly hotter, more profound and less large melted zone.

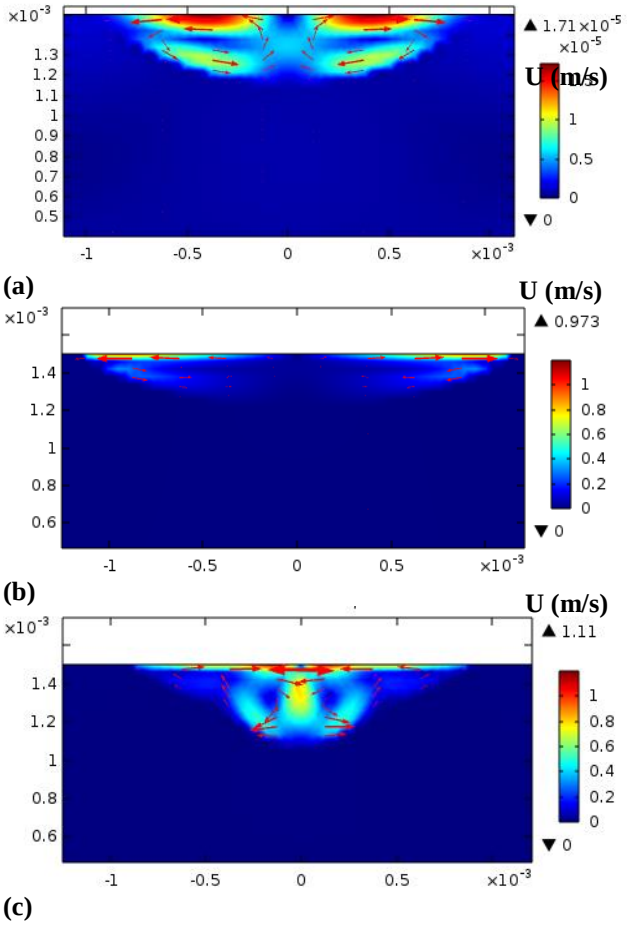

Figure 4. Velocity field (m/s) : (a) natural convection only, (b) natural convection and Marangoni effect with $\gamma = -4 \cdot 10^{-4}$ N/m/K, (c) natural convection and Marangoni effect with $\gamma = 4 \cdot 10^{-4}$ N/m/K.

Table 2. The effect of different convective forces on melting of metal plate with defocused laser (P = 1 kW, Ø = 0.2 cm).

Calculation	T_{max} (K)	Width (mm)	Height (mm)	U_{max} (m/s)
Heat transfer only	1249	2.27	0.43	0
Natural convection	1249	2.27	0.43	$1.71 \cdot 10^{-5}$
Marangoni effect, $\gamma = -4 \cdot 10^{-4}$ N/m/K	1209	2.50	0.39	0.97
Marangoni effect, $\gamma = 4 \cdot 10^{-4}$ N/m/K	1254	2.10	0.49	1.11

Practical work 4 (PW4): simulating the elements transport in multimaterial welding

The last model contains triple multiphysics with time-dependent study (Figure 5):

- heat transfer produced by a pulsed defocused laser, calculated during and after the pulse:

$$Q_{surf} = \frac{a \cdot P}{\pi \cdot R^2} \exp^{\left(-0.5 \cdot \frac{x^2}{R^2}\right)} \cdot \left(t \le t_{pulse}\right)$$

where a – absorption coefficient, t_{pulse} – pulse duration of 0.15 s.

- development and attenuation of natural and Marangoni convection in the melt;
- the mixing of top layer of Ni with base material steel according to Fick law

$$\frac{\partial c}{\partial t} + U \cdot \nabla c = \nabla \cdot \left(D \nabla c\right)$$

where c is the mass fraction of Ni and the diffusion coefficient of Ni in liquid steel D is given by the equation of Stokes-Einstein [6]:

$$D = \frac{k \cdot T}{6 \cdot \pi \cdot \mu \cdot r_{Ni}} \cdot \left(T > T_m\right)$$

where r_{Ni} – the atomic radius of Ni.

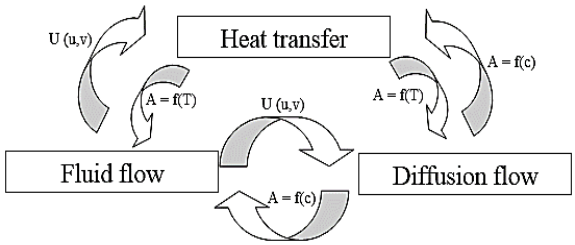

Figure 5. Triple multiphysics scheme.

The 2D geometry of the model represents the cross-section of 304L steel plate (8 wt% Ni) with 500 µm thick pure nickel layer. In such model, the local properties of materials should depend at once on the temperature and on the local mass fraction c of Ni. For simplification, the additivity rule is applied for calculation of local material properties A_i in form:

$$A_i = A_i^{Ni}(T) \cdot c + A_i^{steel}(T) \cdot (1 - c).$$

The calculation time is chosen big enough to witness the whole melting and solidification process (which means, the evolution of solidus line is also estimated with the additivity rule), along with dissolution and mixing of Ni in the melted zone. The students are invited to express the variation of melted zone composition with time and to estimate the influence of γ value on final composition. For the positive value of γ (Figure 6), the progressive dilution of pure nickel in stainless steel is more rapid than in case of negative γ (Figure 7), because of deeper weld penetration, and it also results in lower content of Ni in the final melted zone.

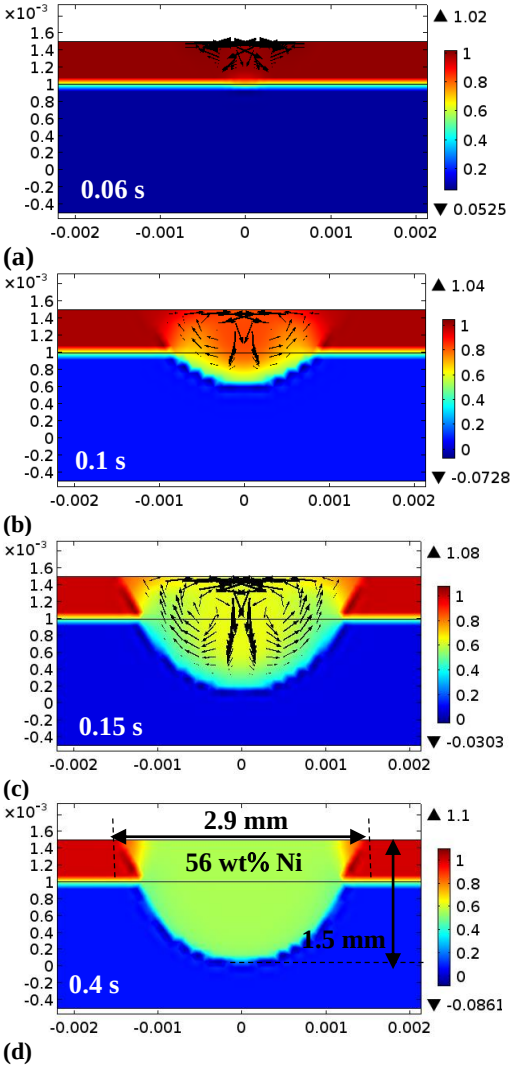

Figure 6. Composition field (wt% Ni) and velocity field (arrows) produced by natural convection and Marangoni effect with $\gamma = 4 \cdot 10^{-4}$ N/m/K.

Discussion

The gradual increase in complexity allows the students to start with simple heat-transfer models and quickly progress up to double and triple multiphysics cases. Because of the limited time, the calculations remain simplified: quasi-steady approaches (PW 1, 2 and 3) or 2D geometry (PW 3 and 4) are applied where possible. In actual form, the module is missing thermomechanical simulation that can be included, for example, in the second practical work that does not contain new theoretical information.

During 3 h session, about 2h are spent on model building and trouble shooting and 1 h on solving and post-processing.

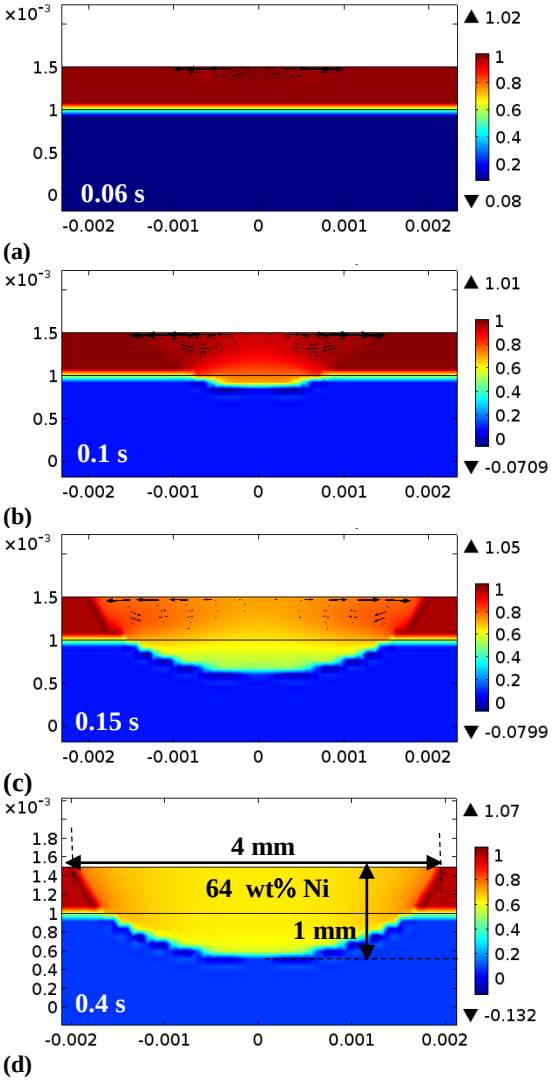

Figure 7. Composition field (wt% Ni) and velocity field (arrows) produced by natural convection and Marangoni effect with $\gamma = -4 \cdot 10^{-4}$ N/m/K.

The analysis of average marks over the last three years (Figure 8.a) shows that that multipysical models (PW 3 and 4) appear more difficult. This is true for both trouble shooting and interpretation of the results. Paradoxically, the general average note slowly diminishes in spite of continuous upgrade of step-by-step manual, and standard deviation does not exceed 2 (Figure 8.b). However, all students appreciate the user-friendliness of COMSOL Multiphysics compared to other FEM software used in materials science and all of them could validate the module by obtaining average mark superior to 10 of 20.Several students decided to use COMSOL Multiphysics for the scientific calculations associated with master internship, and for one student it was imposed.

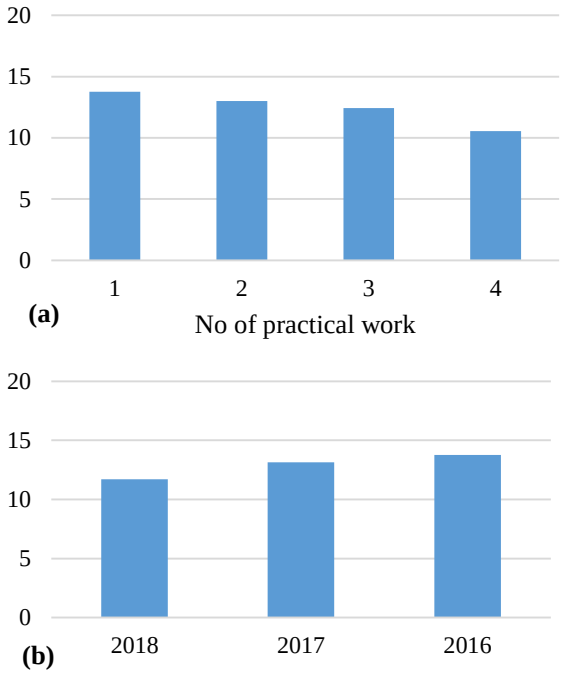

Figure 8. The average marks obtained in last three years (a) for each practical work, (b) for each year.

Conclusions

The use of COMSOL Multiphysics within recently created Master Program «Processes, Controls, Metallic Materials: Nuclear Industry» (PC2M) of University of Burgundy allowed to easily apprehend the main principles of phenomenological simulation of welding process within rather short practical module of 12 h. The gradual increase in complexity allows the students to start with simple heat-transfer models and quickly progress up to double and triple multiphysics cases.

References

1. http://blog.u-bourgogne.fr/master-pc2m/
2. I.Bendaoud, S. Matteï, E. Cicala, I. Tomashchuk, H. Andrzejewski, P. Sallamand, A. Mathieu, F. Bouchaud, The numerical simulation of heat transfer during a hybrid laser–MIG welding using equivalent heat source approach, *Optics & Laser Technology*,**56**, 334-342 (2014).
3. C. Bonacina, G. Comini, A. Fassano, M Primicerio, Numerical solution of phase-change problems, *Int. J. Heat Mass Transfer*, **16**, 1825-1832 (1973).
4. H. Eisazadeh, D. J. Haines, M. Torabizadeh, Effects of gravity on mechanical properties of GTA welded joints, *Journal of Materials Processing Technology*, **214**, 1136-1142 (2014).
5. W. Dong, S. Lu, D. Li, Y. Li, GTAW liquid pool convections and the weld shape variations under helium gas shielding, *International Journal of Heat and Mass Transfer*, **54**, 1420-1431 (2011).
6. C. R. Wilke, Pin Chang, Correlation of diffusion coefficients in dilute solutions, *AIChE Jounal*, **1**, 264-270 (1955).

Acknowledgements

The authors acknowledge the contribution of the students of Master Program PC2M/University of Burgundy, France: Florent Gabard graduated in 2016, Gwendoline Colin graduated in 2017 and Bastien Ravry graduated in 2017.